Case-Control Study

INTERNATIONAL JOURNAL OF SURGERY

OPEN

Early plasma proteomic biomarkers and prediction model of acute respiratory distress syndrome after cardiopulmonary bypass: a prospective nested cohort study

Yu Wang, MD[a,e], Lin Chen, MD[a,e], Chengye Yao, MD[c], Tingting Wang, MD[a,e], Jing Wu, MD[a,e], You Shang, MD[e,d], Bo Li, MD[a,e], Haifa Xia, MD[a,e], Shiqian Huang, MD[a,e], Fuquan Wang, MD[a,e], Shuyu Wen, MD[b], Shaoxin Huang, MD[f], Yun Lin, MD[a,e,*], Nianguo Dong, MD[b,*], Shanglong Yao, MD[a,e,*]

Background: Early recognition of the risk of acute respiratory distress syndrome (ARDS) after cardiopulmonary bypass (CPB) may improve clinical outcomes. The main objective of this study was to identify proteomic biomarkers and develop an early prediction model for CPB-ARDS.

Methods: The authors conducted three prospective nested cohort studies of all consecutive patients undergoing cardiac surgery with CPB at Union Hospital of Tongji Medical College Hospital. Plasma proteomic profiling was performed in ARDS patients and matched controls (Cohort 1, April 2021–July 2021) at multiple timepoints: before CPB (T1), at the end of CPB (T2), and 24 h after CPB (T3). Then, for Cohort 2 (August 2021–July 2022), biomarker expression was measured and verified in the plasma. Furthermore, lung ischemia/reperfusion injury (LIRI) models and sham-operation were established in 50 rats to explore the tissue-level expression of biomarkers identified in the aforementioned clinical cohort. Subsequently, a machine learning-based prediction model incorporating protein and clinical predictors from Cohort 2 for CPB-ARDS was developed and internally validated. Model performance was externally validated on Cohort 3 (January 2023–March 2023).

Results: A total of 709 proteins were identified, with 9, 29, and 35 altered proteins between ARDS cases and controls at T1, T2, and T3, respectively, in Cohort 1. Following quantitative verification of several predictive proteins in Cohort 2, higher levels of thioredoxin domain containing 5 (TXNDC5), cathepsin L (CTSL), and NPC intracellular cholesterol transporter 2 (NPC2) at T2 were observed in CPB-ARDS patients. A dynamic online predictive nomogram was developed based on three proteins (TXNDC5, CTSL, and NPC2) and two clinical risk factors (CPB time and massive blood transfusion), with excellent performance (precision: 83.33%, sensitivity: 93.33%, specificity: 61.16%, and F1 score: 85.05%). The mean area under the receiver operating characteristics curve (AUC) of the model after 10-fold cross-validation was 0.839 (95% CI: 0.824–0.855). Model discrimination and calibration were maintained during external validation dataset testing, with an AUC of 0.820 (95% CI: 0.685–0.955) and a Brier Score of 0.177 (95% CI: 0.147–0.206). Moreover, the considerably overexpressed TXNDC5 and CTSL proteins identified in the plasma of patients with CPB-ARDS, exhibited a significant upregulation in the lung tissue of LIRI rats.

Conclusions: This study identified several novel predictive biomarkers, developed and validated a practical prediction tool using biomarker and clinical factor combinations for individual prediction of CPB-ARDS risk. Assessing the plasma TXNDC5, CTSL, and NPC2 levels might identify patients who warrant closer follow-up and intensified therapy for ARDS prevention following major surgery.

Keywords: ARDS, biomarkers, cardiopulmonary bypass, prediction model, proteomics

[a]Department of Anesthesiology, [b]Department of Cardiovascular Surgery, [c]Department of Neurology, [d]Department of Critical Care Medicine, Union Hospital, Tongji Medical College, Huazhong University of Science and Technology, [e]Key Laboratory of Anesthesiology and Resuscitation (Huazhong University of Science and Technology), Ministry of Education and [f]SpecAlly Life Technology Co., Ltd., Wuhan, Hubei, People's Republic of China

Y.W., L.C., and C.Y. contributed equally to this work as co-first authors.

Sponsorships or competing interests that may be relevant to content are disclosed at the end of this article.

**Corresponding author. Address: Department of Anesthesiology, Union Hospital, Tongji Medical College, Huazhong University of Science and Technology, No. 1277, Jiefang Avenue, Wuhan 430022, People's Republic of China. Tel.: + 861 388 612 8437; Fax; 027-85351653. E-mail: yaoshanglong@hust.edu.cn (S. Yao), and. Tel.: + 861 398 628 8403. E-mail: franklinyun@hust.edu.cn (Y. Lin); Department of Cardiovascular Surgery, Union Hospital, Tongji Medical College, Huazhong University of Science and Technology, No. 1277, Jiefang Avenue, Wuhan 430022, People's Republic of China. Tel.: + 861 597 291 8891. E-mail: dongnianguodoc@hotmail.com (N. Dong)*

International Journal of Surgery (2023) 109:2561–2573

Received 17 January 2023; Accepted 21 April 2023

Supplemental Digital Content is available for this article. Direct URL citations are provided in the HTML and PDF versions of this article on the journal's website, www.lww.com/international-journal-of-surgery.

Published online 1 August 2023

http://dx.doi.org/10.1097/JS9.0000000000000434

Introduction

Innovations, such as the use of more biocompatible surfaces and microcircuits, as well as the increasing expertise of surgeons, anesthesiologists, and perfusionists, have transformed cardiac surgery and cardiopulmonary bypass (CPB) into relatively conventional procedures. Despite these refinements, postoperative organ injuries can present in patients with CPB surgery[1]. Acute respiratory distress syndrome (ARDS) after CPB surgery is associated with a widely variable incidence from 0.4 to 20%[2,3] and a high mortality rate of 80%[4], and there is no specific treatment. No obvious protection can be achieved by ischemic preconditioning[5] or anti-inflammatory treatment[6].

Given that decades of research have failed to find effective therapies for ARDS, the National Heart Lung Blood Institute has recommended that future ARDS research be directed toward identifying patients at high risk[7]. In the past, the prediction model and diagnostic criteria of ARDS were only based on clinical data and physiological variables[8–10]. Methods containing only clinical information fail to meet the needs of ARDS prediction because of the relatively low positive predictive value. Biomarkers may augment prognosis and stratification strategies[11]. For ARDS in acute pancreatitis patients, interleukin-6, interleukin-8, and the systemic inflammatory response syndrome score can be used as comprehensive composite markers to predict the future development of ARDS[12]. Elevated mucin1 levels in plasma had a good predictive value for whether sepsis patients would develop ARDS[13]. Biomarker-directed (tumorigenicity-2 and interleukin-6) ventilator management may improve outcomes in patients with ARDS[14]. Therefore, a comprehensive understanding of the corresponding protein changes in CPB-ARDS may allow patients who are at risk to be identified before progression occurs. Nontargeted proteomics has the potential to identify multiple biomarkers and key pathways of ARDS[15].

In this study, we aimed to compare proteome expression in individuals undergoing cardiac surgery with CPB who do and do not develop ARDS using data-independent acquisition (DIA) proteomics technology and to create a machine learning-based model for the prediction of CPB-ARDS. Furthermore, we explored the dynamic changes in proteins in the lung tissues obtained from rat models of lung ischemia/reperfusion injury (LIRI).

Methods

This prospective observational study has been reported in line with the Strengthening The Reporting Of Cohort Studies in Surgery (STROCSS) Guidelines[16], and the STROCSS checklist is provided in Table A.1 (Appendix A) (Supplemental Digital Content 1, http://links.lww.com/JS9/A835). This study was registered on clinicaltrials.gov (Registration No. NCT04696172) on 6 January 2021 and was approved by the Institutional Review Board of the Wuhan Union Hospital (Approval No. 20200518). The animal experiment protocol was in accordance with the ARRIVE guidelines[17] (Supplemental Digital Content 2, http://links.lww.com/JS9/A836) and was approved by the Experimental Animal Center of Tongji Medical College (IACUC No. 2916).

HIGHLIGHTS

- Plasma thioredoxin domain containing 5 (TXNDC5), cathepsin L (CTSL), and NPC intracellular cholesterol transporter 2 (NPC2) may be predictive biomarkers for acute respiratory distress syndrome (ARDS) after cardiopulmonary bypass (CPB) surgery.
- A parsimonious model based on proteomic and clinical features is developed and validated with excellent performance in predicting CPB-ARDS.
- TXNDC5 and CTSL are upregulated in the lung tissues of lung ischemia-reperfusion injury rats.

Study design

A nested case–control study design was chosen, discovery-based biomarker screening was used in Cohort 1 (April 2021–July 2021, $n = 150$), and validation strategies were used in Cohort 2 (August 2021–July 2022, $n = 375$)[18], at Union Hospital of Tongji Medical College Hospital, a tertiary teaching hospital. Twenty pairs of case–controls in Cohort 1 were selected for perioperative proteomics profile determination and screening of differentially expressed proteins (DEPs) at multiple timepoints. Quantitative analysis and validation of predictive proteins, as well as training and testing of a multimarker prediction model, were carried out within Cohort 2. To assess the external validity of the prediction model, prediction accuracy was determined on Cohort 3 (January 2023–March 2023, $n = 124$). Furthermore, LIRI rat models were established to explore the expression of protein of the lung tissue with the use of proteomics technology, western blotting, and immunofluorescence experiments (Fig. 1).

Study populations and groups

All adult subjects over 18 years old undergoing elective CPB for valves with or without coronary artery surgery were eligible for the study. The exclusion criteria included the following: patients who refuse to sign the informed consent form or the attending physician refuses to allow the patient to join the study; nonelective surgery (surgery at a nonelective time or emergency surgery); preoperative pulmonary insufficiency, pulmonary hypertension, and pulmonary inflammation; the absence of any specimen and clinical data; and patients who had a failed operation, needed extracorporeal membrane oxygenation support, or underwent CPB operation again within 3 days after operation.

Patients who developed ARDS in the first 3 days after CPB were placed into the ARDS group. In Cohort 1 for the proteomics analyses, once the case was determined, an additional patient was matched as a control in the non-ARDS patient group based on the following criteria: same group of surgeons; same type of operation; same sex; and the differences of BMI and age were within $\pm 10\%$ compared with the ARDS patient[19]. In Cohort 2, for the development of the prediction model and to fully consider the prediction contribution of clinical factors, the controls were only matched by the same group of surgeons and randomly selected from non-ARDS patients (case:control = 1:2). Multiple clinical variables and protein variables were included in the multivariable logistic regression.

The sample size for the development of the final multivariable logistic regression should be more than 20 times the number of

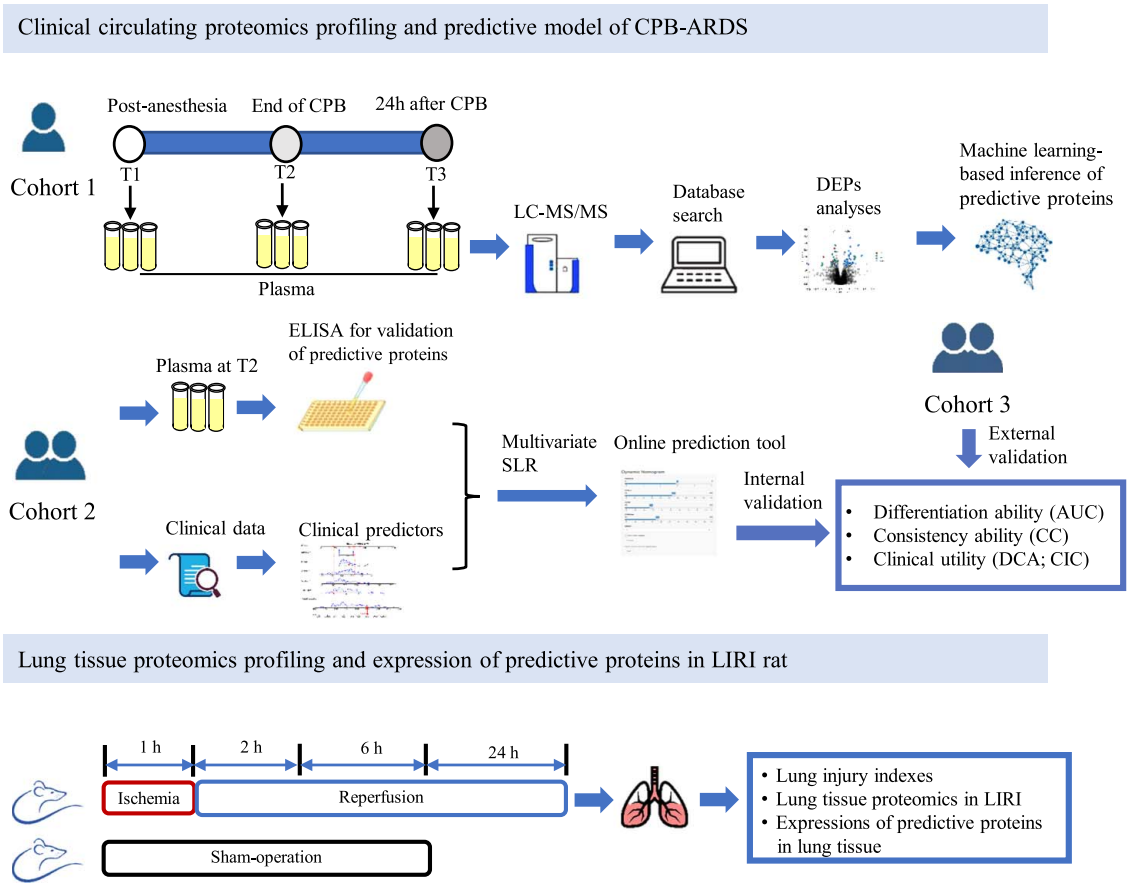

Figure 1. Study design and flow chart. AUC, area under the receiver operating characteristic curve; CC, calibration curve; CIC, clinical impact curve; CPB-ARDS, cardiopulmonary bypass induced acute respiratory distress syndrome; DCA, decision curve analysis; DIA, data-independent acquisition; DEPs, differentially expressed proteins; ELISA, enzyme-linked immunosorbent assay; LIRI, lung ischemia/reperfusion injury; LC–MS/MS, liquid chromatography–mass spectrometry; SLR, stepwise logistic regression algorithm.

predictors to efficiently avoid over fitting. All participants underwent CPB under total intravenous general anesthesia and were admitted to the cardiac surgery intensive care unit (CICU). The standardized CPB operation, anesthesia and ventilation protocol, and postoperative treatment procedures of the patients are shown in Method A.1 (Appendix A) (Supplemental Digital Content 1, http://links.lww.com/JS9/A835).

Clinical data and outcome data collection

Potential perioperative ARDS clinical risk factors that have been reported in previous studies were collected by trained investigators[8,9,20–22]. The clinical variables were collected from preoperation to the end of the CPB operation, only representative indicators for prediction before the onset of ARDS were considered[23]. The following data were included (please refer to Method A.2 for details, Supplemental Digital Content 1, http://links.lww.com/JS9/A835): (1) demographic information and preoperative complications; (2) preoperative laboratory values; (3) CPB surgery-related variables, including intraoperative infusion; anesthesia time; CPB time; electric defibrillation, ultrafiltration volume, precharge fluid volume, additional fluid volume, cardioprotective fluid volume; (4) blood transfusion: volume of red blood cell transfusion; volume of plasma transfusion; volume of platelet transfusion; and massive transfusion of red blood cells (MRBC).

The primary outcome variable was the development of ARDS within 3 days after CPB. Based on the Berlin definition[10], ARDS was independently confirmed by two physicians who reviewed the medical records (Method A.3, Supplemental Digital Content 1, http://links.lww.com/JS9/A835). Chest radiograph of these patients were performed daily or twice per day. Blood gases were examined every 4–6 h. Respiratory failure in patients with ARDS was not fully explained by cardiac failure or fluid overload and was evaluated twice from echocardiography, clinical symptoms, and other indicators.

DIA proteomic analyses and validation

Blood samples were obtained from all consecutive patients included in the cohort at three timepoints: prior to CPB after anesthesia induction (T1), immediately after CPB (T2), and 24 h after CPB (T3). All blood samples were collected from the artery and centrifuged at 3000*g* for 15 min, and the supernatants were aliquoted and stored at – 80°C. After the outcome of the patients in the cohort was determined through follow-up, plasma samples of the case and control groups were used for DIA proteomic techniques and enzyme-linked immunosorbent assay (ELISA)

analyses within 6 months after collection. No more than two freeze–thaw cycles were permissible for each sample.

The laboratory procedures were conducted blind to the case–control status. After liquid chromatography–mass spectrometry (LC–MS/MS) analysis, raw MS data were searched using MSFragger software (Method A.4, Supplemental Digital Content 1, http://links.lww.com/JS9/A835). The searched results were filtered with 1% FDR at both the protein and peptide levels. The missing values of protein abundance were filled with half of the global minimum and half of the peptide minimum according to random tail imputation[24].

In an effort to reproduce our findings, ELISA analyses for the targeted DEPs were conducted in a new group of patients within Cohort 2. Four protein predictors, cathepsin L (CTSL) (MBS7254442, MyBioSource, Inc.), thioredoxin domain containing 5 (TXNDC5) (abx382455, Abbexa, Inc.), NPC intracellular cholesterol transporter 2 (NPC2) (SEK13341, Sino Biological), and neural cell adhesion molecule 1 (CD56) (abx573795, Abbexa), in the plasma at T2 were detected, as per the manufacturer's instructions. Details about the ELISA are provided in Method A.5 (Supplemental Digital Content 1, http://links.lww.com/JS9/A835).

Animal surgery and experimental protocol

LIRI is the most common lung injury in CPB–associated lung injury during cardiac surgery[25]. The LIRI rat models were established by the left hilar clamp as previously published[26]. Fifty male Sprague Dawley (SD) rats ((Beijing Vital River Laboratory Animal Technology Co., Ltd. ; Certificate number SYXK2021-0011), weighing 300±20 g, were randomly divided into four groups: sham group ($n=16$), ischemia–reperfusion for 2 h group ($n=9$), ischemia–reperfusion for 6 h group ($n=16$) and ischemia–reperfusion for 24 h group ($n=9$). The number of animals for different experimental procedures at different timepoints after reperfusion is summarized in Method A.6 (Supplemental Digital Content 1, http://links.lww.com/JS9/A835). After reperfusion, left lung tissue and serum were obtained. The severity of lung injury was scored using a semiquantitative scoring system as described previously[27,28]. Please refer to Method A.6 (Supplemental Digital Content 1, http://links.lww.com/JS9/A835) for further details.

Protein analyses of rat lung samples

For the proteomic profile at the tissue level for certain LIRI groups, LC–MS/MS experiment-based proteomic analyses were conducted on the lung samples of the LIRI and sham rats. Upon identifying CPB-ARDS circulating predictive proteins in the clinical cohorts, we compared the tissue-level expression of these proteins in the LIRI and sham groups (1) by incubating frozen lung tissue homogenate with primary specific antibodies and performing Western blotting and (2) by comparing the protein expression in lung tissue with immunofluorescence staining and confocal microscopy (Nikon A1R).

Statistics

Screening of DEPs and predictive proteins in Cohort 1

For circulating proteomic data from Cohort 1, the fold change (FC) value was calculated based on the ratio of ARDS/non-ARDS. The statistical significance was calculated for proteins using the paired two-sided *t*-test ($P<0.05$)[29]. DEPs were defined as those with a significant difference between ARDS and non-ARDS (*P*-value <0.05, and $|\log_2(FC)| > 0.263$). To further investigate potential pathological and biological mechanisms relevant to CPB-ARDS, we performed Gene Ontology (GO)/Kyoto Encyclopedia of Genes and Genomes (KEGG) enrichment and protein–protein interaction (PPI) analyses (Method A.7, Supplemental Digital Content 1, http://links.lww.com/JS9/A835)

The Least Absolute Shrinkage and Selection Operator (LASSO) regression and the extreme gradient boosting (XGBoost) model were used to screen predictive protein features from the DEPs. The DEPs were sorted according to the importance score (gain percent). DEPs with gain percentages greater than 10% were included as candidate predictive proteins for subsequent modeling.

Development and validation of a prediction model in Cohorts 2 and 3

The distribution differences of clinical features were compared using Student's/Welch's *t*-test or Wilcoxon rank sum exact test for continuous variables and Pearson's χ2-test or Fisher's exact test for categorical variables among the CPB-ARDS and non-ARDS groups from Cohort 2. Then, the clinical variables with $P<0.05$ were entered into a stepwise logistic regression algorithm (SLR) to screen clinical predictors and develop the clinical prediction model.

For the collection time of samples, the earlier collection of samples in the development of ARDS may deduce the biological signals of ARDS in a timely manner and enhance efforts to prevent and intervene[30]. Considering that time point T2 was immediately after the CPB injury and before the occurrence of ARDS, DEPs at T2 may be more conducive to the prediction of the early stages of ARDS. Then, quantitative analyses were conducted to validate the differential expression of the candidate predictive proteins at T2.

Finally, the protein predictors and the screened clinical predictors were combined to construct the combined CPB-ARDS prediction score (CAPS) model. An interactive web-based dynamic nomogram application was built with Shiny, version 0·13·2·26. In addition, the nomogram was subjected to 3-fold, 5-fold, and 10-fold cross-validation for internal validation to assess its predictive accuracy. The CAPS model was evaluated from three aspects: model differentiation ability (receiver operating characteristic curve, ROC), consistency (calibration curve), and clinical utility (decision curve analysis, DCA; clinical impact curve, CIC). We further calculated the sensitivity, specificity, precision, and F1 score to evaluate the ability of the models. Specific calculation methods are shown in Method A.8 (Supplemental Digital Content 1, http://links.lww.com/JS9/A835). To externally validate the results, the cumulative points of each patient in the validation cohort (Cohort 3) were computed based on the final model established using the training dataset (Cohort 2). Subsequently, a SLR was performed using the cumulative points as a factor, and finally, the ROC and calibration curve were derived and reported.

All assessments of predictors were conducted blind to the case–control status. All computations were conducted in the R environment, version R version 4·2·0 (April 2022). The results with $P \leq 0{\cdot}05$ were considered statistically significant.

Results

Study design and patients

For the proteomic profiling and protein biomarker discovery study, plasma samples of 20 CPB-ARDS and 20 matched non-ARDS patients within Cohort 1 (150 patients) underwent LC–MS/MS-based proteomic analyses. In Cohort 2 (375 patients), 50 CPB-ARDS and 100 randomly selected non-ARDS patients (case: control = 1:2) were included for biomarker validation and the establishment of the prediction model. In Cohort 3 (124 patients), 20 CPB-ARDS and 20 randomly selected non-ARDS patients were included for external validation of the prediction model (Fig. 1). The specific screening process and numbers that signified potentially eligible, examined for eligibility, and confirmed eligible, that were included in the study, completed during follow-up, and analyzed in Cohorts are all shown in Figure A.1 (Appendix A), Supplemental Digital Content 1, http://links.lww.com/JS9/A835.

Altered plasma proteomic profiling in the perioperative period of CPB-ARDS

The clinical characteristics of the patients for proteomic profiling are recorded in Table A.2 (Supplemental Digital Content 1, http://links.lww.com/JS9/A835). Compared with the CPB-ARDS group, the difference in clinical factors in the non-ARDS group after random matching was not statistically significant. For the 120 plasma samples from Cohort 1 at three timepoints, we obtained 6284 peptides, and 709 human proteins were quantified. All proteins are shown in Table A.3 (Supplemental Digital Content 1, http://links.lww.com/JS9/A835) with normalized expression values. The total sample protein, peptide overview, and more details on the quality control and analysis of the proteomics results are presented in Figure A.2 (Supplemental Digital Content 1, http://links.lww.com/JS9/A835). Furthermore, principal component analyses showed the spatial distribution of the quantitative information of two groups of proteins, indicating the protein alterations in CPB-ARDS patients against non-ARDS (Fig. A.3, Supplemental Digital Content 1, http://links.lww.com/JS9/A835). The volcano plots showed the molecular alterations of 9, 29, and 35 proteins in CPB-ARDS versus non-ARDS patients at T1, T2, and T3, respectively (Fig. 2 A, B, C;F, C and *P*-values are shown in Table A.4, Supplemental Digital Content 1, http://links.lww.com/JS9/A835). The quantitative differences in DEPs among each sample from the CPB-ARDS and non-ARDS groups are shown in the heatmap (Fig. A.4, Supplemental Digital Content 1, http://links.lww.com/JS9/A835).

The PPI network based on the String/Genemania database and enriched GO/KEGG pathways after CPB (at T2 and T3) were analyzed. Neutrophil degranulation (GO: 0043312) and neutrophil activation involved in the immune response (GO: 0002283) were the top enriched biological processes at both T2 and T3 (Fig. 2 D, G; the gene-ratio and the adjusted *P*-value of the top 5 terms are shown in Tables A.5 and 6). The key node proteins in the PPI network based on the String database after CPB (T2 and T3) were involved in biological processes related to neutrophil immunity (Fig. 2 F, I) (combined score and degree are shown in Table A.7, Supplemental Digital Content 1, http://links.lww.com/JS9/A835). Moreover, these DEPs frequently interacted with one another in PPI networks from the Genemania database at T2 and T3 (Fig. 2 E, H). Coexpression, colocalization, and physical interactions were the major PPI modes among DEPs after CPB. The PPI network and enriched GO/KEGG pathways before CPB (at T1) are shown in Figure A.5 (Supplemental Digital Content 1, http://links.lww.com/JS9/A835).

Machine learning-based inference of biomarkers

For proteomic data and by using LASSO regressions, 8, 18, and 7 DEPs were identified as candidate features for XGBoost models at T1, T2, and T3, respectively (Fig. A.6, Supplemental Digital Content 1, http://links.lww.com/JS9/A835). According to the feature contributions calculated by the XGBoost model for proteins at the end of CPB (T2), the 11 most important protein features were obtained, which could distinguish CPB-ARDS and non-ARDS (Fig. 3). The top four protein features were considered candidate biomarkers for the prediction of CPB-ARDS, including NPC2, CD56, TXNDC5, and CTSL, with gain percentages exceeding 10%. XGBoost analyses for predictive protein features were also obtained at T1 and T3, which are shown in Figure A.7 (Supplemental Digital Content 1, http://links.lww.com/JS9/A835) and Figure A.8 (Supplemental Digital Content 1, http://links.lww.com/JS9/A835). The weight ranking features of the three XGBoost models are summarized in Table A.8 (Supplemental Digital Content 1, http://links.lww.com/JS9/A835).

Validation of expressions of the biomarker changes

The protein markers at the end of CPB (T2) may be more relevant to CPB-related lung injury and conducive to the prediction of the early stage of CPB-ARDS. Therefore, the top four protein biomarkers in the XGBoost model at T2 were selected for quantitative verification by ELISA in another independent cohort. Three proteins (TXNDC5, CTSL, and NPC2) showed statistically significant differences between CPB-ARDS and non-ARDS patients within Cohort 2, except CD56 (Fig. 4A–D). Univariable logistic regression showed that high concentrations of TXNDC5, CTSL, and NPC2 were associated with a high risk of ARDS (Table A.9, Supplemental Digital Content 1, http://links.lww.com/JS9/A835). We next determined whether altered plasma levels of TXNDC5, CTSL, and NPC2 were related to the reduction in PaO_2/FiO_2 (PF ratio) and the extension of intubation retention time as a consequence of CPB surgery. The Spearman correlation coefficient results showed that the expression levels of NPC2, TXNDC5, and CTSL were positively correlated with the intubation retention time (Fig. 4E–G) and negatively correlated with the minimum PF ratio (Fig. 4H–J).

Nomogram-based prediction model for CPB-ARDS

The clinical characteristics of the 150 patients in Cohort 2 are reported in Table 1. After preliminarily testing the differences among the CPB-ARDS and non-ARDS groups within Cohort 2, the clinical factors with *P*-values <0.05 included age, anesthesia time, CPB time, ultrafiltration volume, cardioprotective fluid volume, volume of plasma transfusion, and MRBC. After multivariable SLR, MRBC, CPB time, age, and ultrafiltration volume constituted a clinical prediction model (Fig. A.9, Supplemental Digital Content 1, http://links.lww.com/JS9/A835), with an AUC (area under the receiver operating characteristic curve) of 0.767. The SLR coefficient results showed that MRBC and CPB time were statistically significant clinical predictors (Table A.10, Supplemental Digital Content 1, http://links.lww.com/JS9/A835).

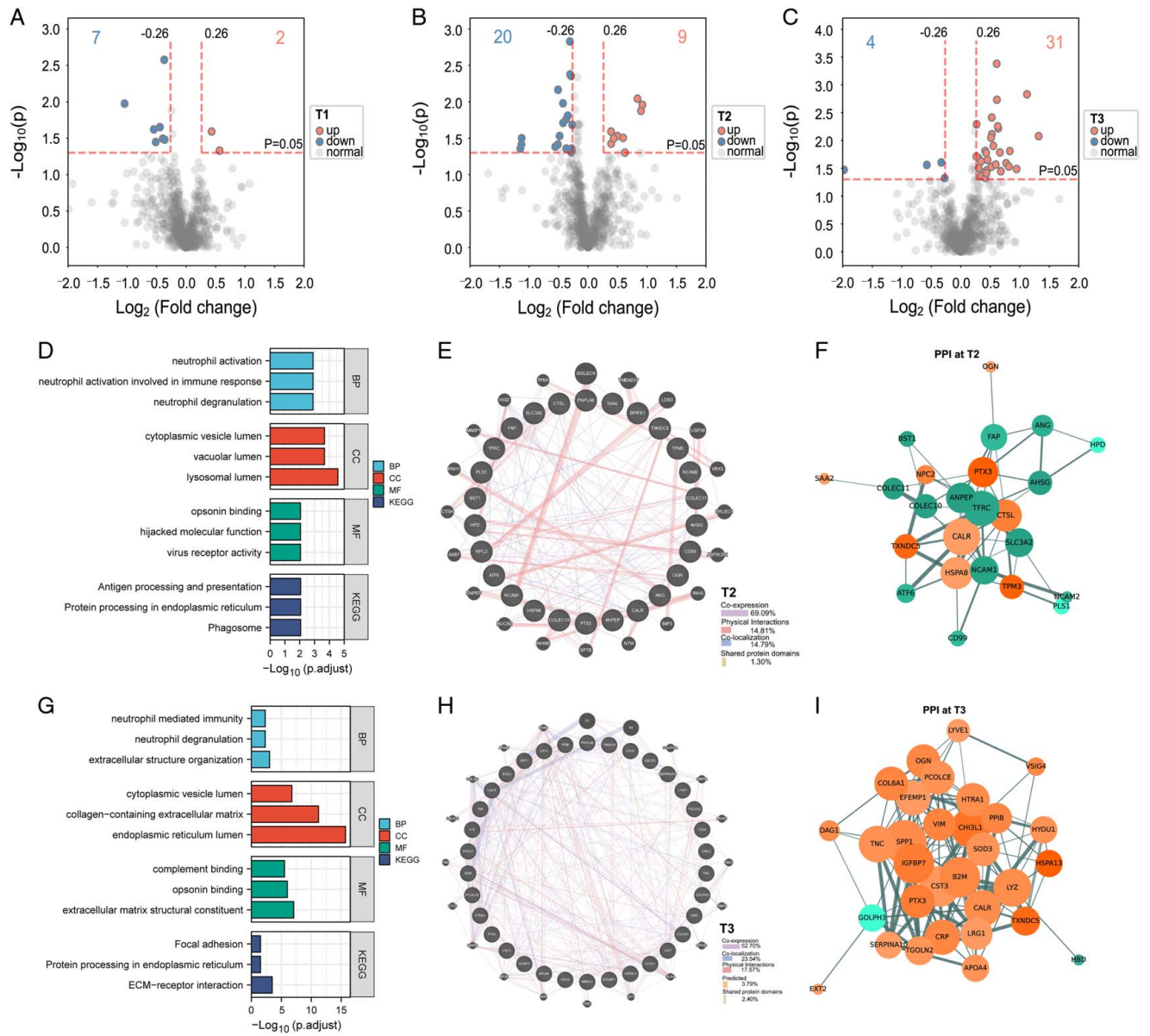

Figure 2. The DEPs among CPB-ARDS and Non-ARDS patients in Cohort 1. The volcano plot of protein expression in CPB-ARDS patients compared to Non-ARDS patients at T1 (A), T2 (B), and T3 (C); The top three GO and KEGG enriched items at T2 (D), and T3 (G); The PPI networks from Genemania database at T2 (E), and T3 (H); The PPI networks from String database at T2 (F), and T3 (I).

For the development of the combined prediction model, three significantly altered proteins (TXNDC5, CTSL, and NPC2) and two significant clinical predictors (MRBC and CPB time) were reserved as a candidate pool. The number of protein and clinical predictors is 5, which is less than 1/20 of the sample size, and could efficiently avoid overfitting. After the SLR, the CAPS model was developed as a simple-to-use nomogram (Fig. 5A). In addition, we built an operation interface on a web page (https://wy-wuhanunion.shinyapps.io/CAPS_DynNomapp_WY/) to calculate the probability of CPB-ARDS (Fig. A.10, Supplemental Digital Content 1, http://links.lww.com/JS9/A835). By entering a patient's clinical characteristics and concentration of target proteins, the user can obtain the predictive probability of CPB-ARDS. The adjusted parameters of the proteins and clinical predictors in the CAPS model are presented in Table A.11 (Supplemental Digital Content 1, http://links.lww.com/JS9/A835).

The corresponding ROC curves showed that the AUC of the CAPS was higher than that of the clinical model (0.852 vs. 0.767, *P*-value =0.024), suggesting a better performance in discrimination (Fig. 5B). The internal validation of the nomogram was performed with 3-fold, 5-fold, and 10-fold cross-validations, and the AUC of the CAPS model was also more than 0.830 (Table 2). CAPS also exhibited reliable calibration performance, as evidenced by a Brier Score of 0.136 (95% CI: 0.102–0.170) (Fig. 5C). The CAPS showed good performance, with a precision of 83.33%, a sensitivity of 93.33%, a specificity of 61.16%, and an F1 score of 85.05%

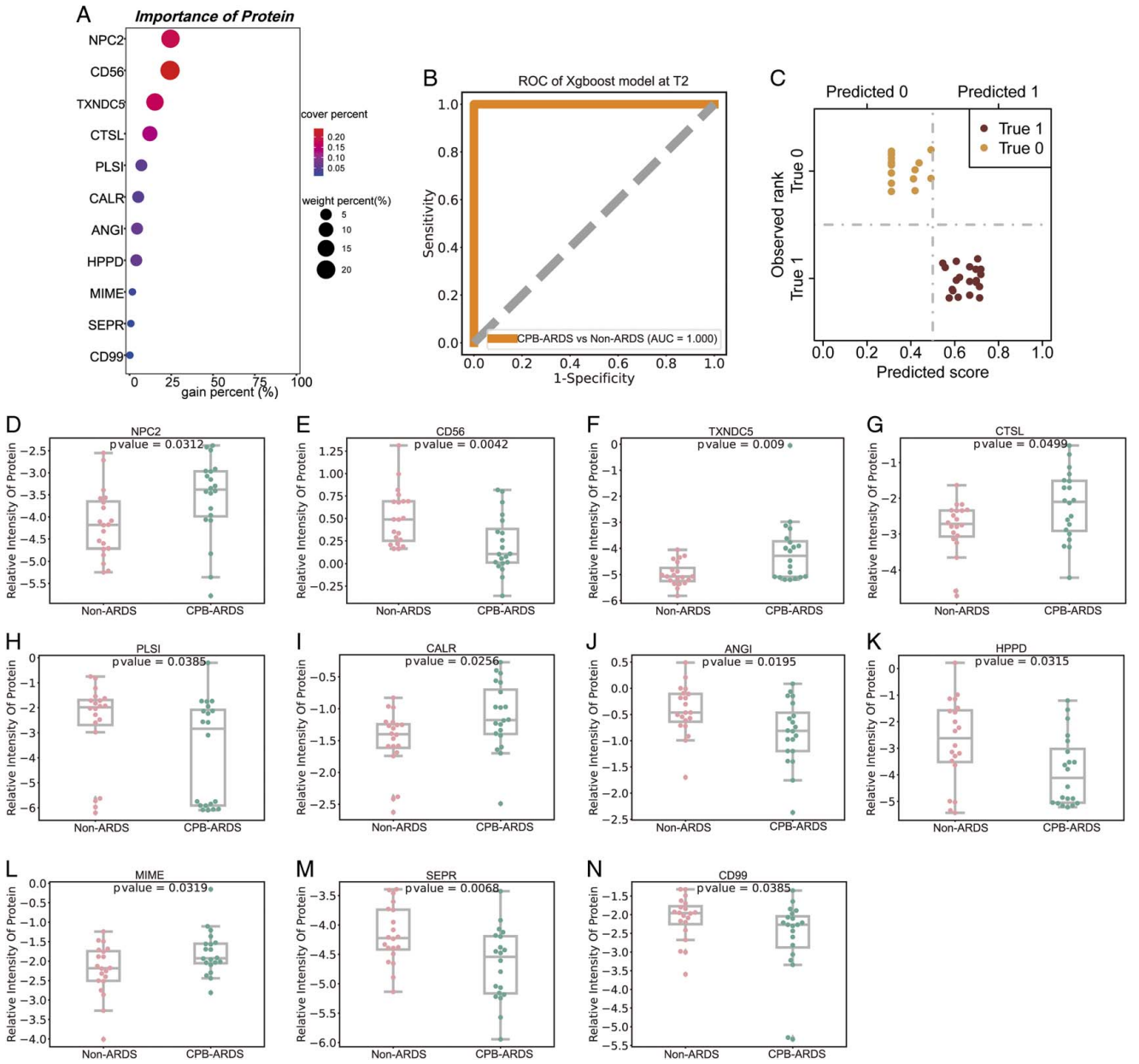

Figure 3. The machine learning-based inference of biomarkers strongly altered at the end of CPB in Cohort 1. The XGBoost results for protein features at T2 (A); Receiver operating characteristic curve (B); Confusion matrix (C); The relative intensity of 11 protein features among Non-ARDS and CPB-ARDS groups at T2 (D–N). ROC, receiver operating characteristic curve.

(Table 2). According to the DCA of the two prediction models, the net benefit for the CAPS model was larger than that for the traditional clinical model (Fig. 5D). CIC analysis of CAPS visually showed that the nomogram had a superior overall net benefit within the wide ranges of the threshold probabilities and impacted patient outcomes (Fig. 5E). External validation performance on Cohort 3 was maintained in model discrimination with an AUC of 0.820 (95% CI: 0.685–0.955) (Fig. 5F), and calibration with a Brier Score of 0.177 (95% CI: 0.147–0.206) (Fig. 5G). The data of predictors in the validation dataset are reported in Table A.12 (Supplemental Digital Content 1, http://links.lww.com/JS9/A835).

Altered expression of proteins in lung tissues from LIRI rats

To gain insight into the function of the three protein predictors in LIRI injury and the protein expression in lung tissue, molecular biology approaches were used in the LIRI rat model. First, male SD rats were randomly assigned to four groups to observe the temporal trend of lung injury after ischemia–reperfusion. H&E staining showed lung injury after 2, 6, and 24 h of reperfusion (Fig. 6A). In addition, the lung injury score and number of inflammatory cells after 6 h of reperfusion were higher (Fig. 6B, C). Moreover, we found an imbalance in oxidative stress mediators and inflammatory markers (Fig. A.11, Supplemental Digital Content 1, http://links.

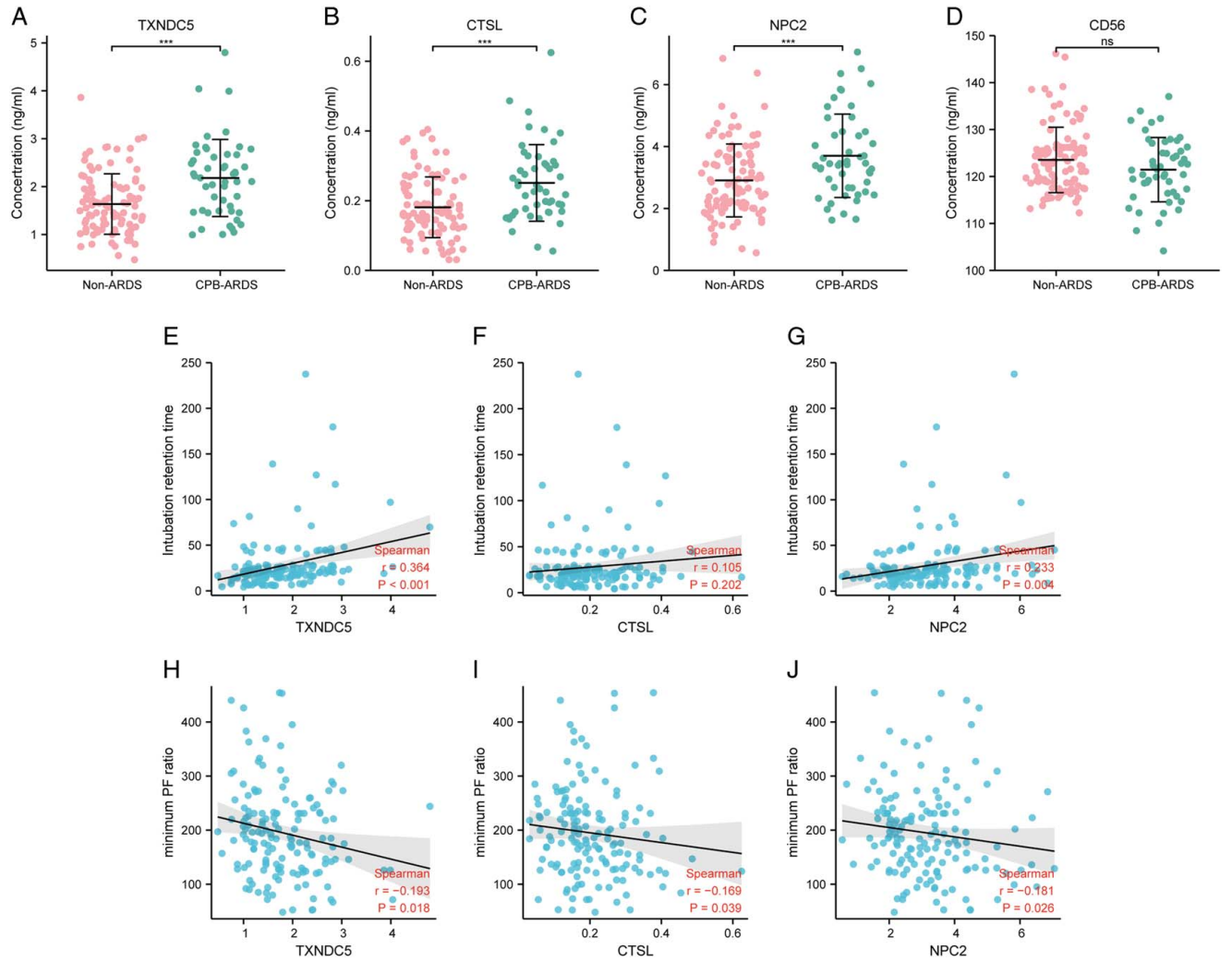

Figure 4. ELISA analyses for the targeted proteins and the correlation of the protein concentration with values of a panel of clinical parameters in Cohort 2.The targeted protein concentration among CPB-ARDS and Non-ARDS patients for TXNDC5 (A), CTSL (B), NPC2 (C), and CD56 (D); The results of spearman correlation analyses of concentration of TXNDC5 (E), CTSL (F), NPC2 (G) and intubation retention time; The results of spearman correlation analyses of concentration of TXNDC5 (H), CTSL (I), NPC2 (J) and minimum PF ratio. PF ratio, PaO_2/FiO_2.

lww.com/JS9/A835) after 6 h of reperfusion. The downregulation of Occludin and ZO-1 protein (Fig. 6E) as well as the higher leakage of Evans blue (Fig. A.12, Supplemental Digital Content 1, http://links.lww.com/JS9/A835), indicated serious damage to the blood-gas barrier after 6 h of reperfusion.

We therefore conducted an LC–MS/MS-based proteomic analyses for proteomic profiling at the tissue level with rat lung samples of LIRI after 6 h of reperfusion and sham groups. For the 3 protein predictors of the CAPS model in the clinical cohorts, CTSL and TXNDC5 were also significantly upregulated in the LIRI lung tissue proteomic results (Fig. 6F). Immunoblot and immunofluorescence analyses showed that the dysregulation of CTSL and TXNDC5 in the LIRI lung tissue was consistent with the proteomic data (Fig. 6I–L).

Discussion

Our integrative clinical and animal experimental study reveals the vital role and clinical relevance of CTSL, TXNDC5, and NPC2 during CPB-related lung injury, and a novel prediction model of CPB-ARDS is established and validated with protein biomarkers and clinical features.

First, a nontargeted proteomics study identified DEPs at multiple timepoints; then, the targeted proteins at the end of CPB were validated in a new cohort, in which CTSL, TXNDC5, and NPC2 emerged as strong predictors of ARDS within 3 days after CPB operation. The CAPS model combining clinical and protein data was established for the prediction of ARDS after CPB surgery. The final model generally validated well in both internal and external validation. Furthermore, the LIRI rat model confirmed increased levels of CTSL and TXNDC5 protein in the lung tissue in the proteomic, immunoblot, and immunofluorescence analyses, suggesting that loss-of-function or gain-of-function experiments are needed to demonstrate that the protein predictors are potential regulators in CPB-related lung injury.

Traditional studies in ARDS treatment typically identify and recruit patients well into the exudative phase of ARDS, a point

Table 1

Clinical factors among CPB-ARDS and non-ARDS patients within Cohort 2.

[a]Variables	CPB-ARDS group ($n=50$)	Non-ARDS group ($n=100$)	[b]*P*
Demographic information and preoperative complications			
Age	62.0 (56.3, 66.0)	59.0 (50.0, 64.0)	**0.046**
Sex (male%)	34 (68.0%)	59 (59.0%)	0.372
BMI	23.1 ± 3.0	23.1 ± 2.6	0.421
Smoking	16 (32.0%)	23 (23.0%)	0.324
Alcohol	12 (24.0%)	22 (22.0%)	0.945
Hypertension	23 (46.0%)	31 (31.0%)	0.104
Diabetes	5 (10.0%)	3 (3.0%)	0.158
Stroke	10 (20.0%)	11 (11.0%)	0.212
Preoperative laboratory values			
Hematocrit	39.6 (35.6, 42.0)	39.2 (35.1, 41.9)	0.674
Hemoglobin	131.0 (120.3, 141.0)	129.0 (114.8, 138.0)	0.405
White blood cell count	5.5 (4.4, 6.5)	5.4 (4.5, 6.6)	0.957
Albumin	38.8 (36.6, 40.3)	38.4 (36.6, 40.4)	0.889
ALT	22.0 (15.3, 37.5)	24.0 (15.0, 43.0)	0.829
AST	25.5 (19.0, 40.3)	22.5 (18.0, 31.0)	0.205
Creatinine	78.4 (66.0, 86.1)	72.0 (62.7, 86.2)	0.251
CPB-related variables			
[c]Surgery type (Complex%)	36 (72.0%)	57 (57.0%)	0.108
Input volume	1850 (1500, 2160)	1750 (1500, 2000)	0.531
Anesthesia time	393.0 (326.3, 507.8)	370.0 (322.5, 402.0)	**0.041**
CPB time	163.5 (113.8, 203.3)	108.5 (91.0, 141.0)	**< 0.001**
Electric defibrillation	19 (38.0%)	27 (27.0%)	0.234
Ultrafiltration volume	2450 (1550, 3425)	2000 (1400, 2500)	**0.009**
Precharge fluid volume	1100 (1000, 1100)	1100 (1000, 1162)	0.930
Additional fluid volume	0.0 (0.0, 171.9)	0.0 (0.0, 143.8)	0.570
Cardioprotective fluid volume	1800 (1400, 2200)	1500 (1400, 1800)	**0.016**
Urine volume	1675 (1112, 2287)	1400 (1050, 1900)	0.166
Blood transfusion			
Transfusion reaction	6 (12.0%)	19 (19.0%)	0.394
Volume of RBC transfusion	4.5 (2.0, 5.0)	4.0 (2.0, 5.6)	0.067
Volume of plasma transfusion	500.0 (350.0, 887.5)	375.0 (200.0, 600.0)	**0.002**
Volume of platelet transfusion	0.0 (0.0, 1.0)	0.5 (0.0, 1.0)	0.087
MRBC	31 (62.0%)	32 (32.0%)	**< 0.001**
Secondary outcome			
Minimum PF ratio	28.2 (23.6, 46.9)	16.8 (9.8, 20.8)	< 0.001
Intubation retention time	126.0 (92.5, 154.0)	220.5 (176.8, 271.3)	< 0.001

[a]Descriptive statistics are reported as mean ± SD or median (lower quartile, upper quartile) for continuous variables, and as frequency (percentage) for categorical variables.
[b]Comparison of the two groups was performed using the Student's/Welch *t*-test or Wilcoxon rank sum exact test for continuous data; Pearson's $\chi 2$-test or Fisher's exact test for categorical data.
[c]Complex surgery includes multivalvular surgery, or valvular surgery combined with coronary artery surgery.
ALT, alanine aminotransferase; AST, aspartate aminotransferase; CPB, cardiopulmonary bypass; MRBC, massive transfusion of red blood cells; PF, PaO_2/FiO_2; RBC, red blood cells.

at which the trajectory of lung injury may be either irreversible or at least extremely difficult to modify. Importantly, ARDS prevention measures must start earlier – in the emergency or operating room for patients undergoing CPB who are at great risk of ARDS. The prediction system in our study was comprised of two parts: one focused on perioperative clinical risk factors, one on easily available biomarkers (plasma proteome). Previous studies on ARDS prediction only focused on clinical risk factors and physiologic markers, including the Lung Injury Prediction Score (LIPS)[23] and Surgical LIPS[31]. Moreover, due to different target populations, diagnostic criteria, and risk factors, the previous prediction score of ARDS (such as LIPS, surgical LIPS, etc.) may not be fully applicable to the prediction of ARDS in patients with special surgery, such as CPB-ARDS. We developed the CAPS model that combined proteins and the typical clinical factors of CPB-ARDS reported in previous studies, and compared this model to the model with typical clinical factors alone. Protein biomarkers could theoretically improve ARDS prediction, but a pragmatic approach incorporating both clinical and protein variables has yet to be developed, especially for postoperative ARDS. Combining angiopoetin-2 with LIPS resulted in a modest improvement in predicting subsequent ARDS compared to either method alone (AUC 0.84 versus 0.74)[32]. The combination of serum Parkinson's disease 7 and clinical prediction scores ameliorated the prediction accuracy for ARDS in populations with severe sepsis/septic shock[33]. Compared with the prediction model based on the typical clinical risk factors alone that was established in our study, the CAPS model also showed an improvement in discrimination performance (AUC: 0.852 vs. 0.767, *P*-value = 0.024) and clinical benefit from the DCA results. Furthermore, the CAPS model exhibited good external validity by reproducing its predictive performance in an independent external dataset. The discriminative ability of the model as measured by the AUC was fair and very close to that reported in the development study. The small decrease in the AUC was expected as we applied an existing prediction model in a new population. Brier Scores, which are under 0.25, indicated reasonable calibration in both the development and the validation cohort. These results suggest that the model performed well in the development dataset may also be applicable to other populations, and be generalizable to a range of postoperative care settings following CPB surgery.

On the other hand, the unique and novel prediction ability of TXNDC5, CTSL, and NPC2 may enrich our understanding of the pathogenesis of CPB-ARDS. Recent studies have reported the dual role of TXNDC5 as a novel biomarker and mediator in multiorgan fibrosis, including pulmonary fibrosis[34] and cardiac fibroblasts[35]. TXNDC5 is highly upregulated in both human and mouse fibrotic lungs and promotes pulmonary fibrosis by enhancing TGFβ signaling activity[34]. However, evidence on the molecular role of TXNDC5 in ARDS is sparse. In the current study, high levels of TXNDC5 were found in the plasma of ARDS patients after CPB, and in the lung tissue of rats after ischemia/reperfusion.

The circulating and tissue levels of CTSL were elevated after SARS-CoV-2 infection[36], suggesting that CTSL is likely to be a potential therapeutic target for blocking viral entry[36,37]. CTSL has been linked to IR injury, including renal IR injury[38] and myocardial IR injury[39]. Consistent with previous studies, we also reported the crucial role of CTSL in the plasma of CPB-ARDS patients and the lung tissue of LIRI rats.

NPC2 is a small glycoprotein resulting from mutations in the NPC2 gene that lead to an abnormal increase in intracellular cholesterol[40]. A recent quantitative proteomic analysis showed a significant increase in the level of plasma NPC2 in pneumonia patients, sepsis patients, and patients who subsequently developed septic shock or died within 30 days[41]. Our data showed a significant accumulation of NPC2 after CPB in

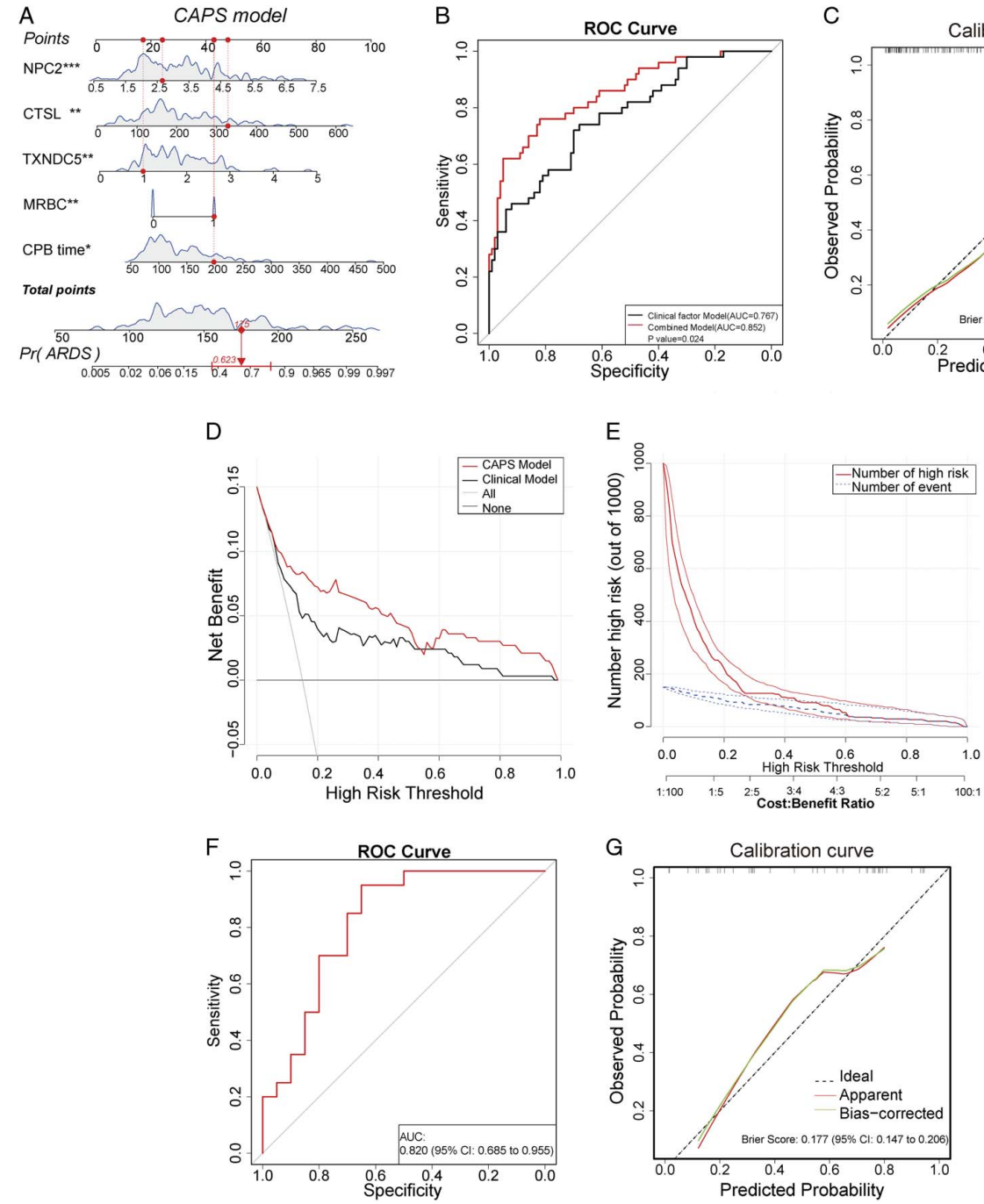

Figure 5. Nomogram-based CAPS prediction model for CPB-ARDS. The nomogram of CAPS composed of clinical and protein factors at T2 in Cohort 2 (A). Draw a vertical line from the corresponding axis of each factor to the points axis to acquire the point of this factor. Make a summation of the points for each factor to yield a total score, and the probability of CPB-ARDS could be estimated by projecting the total score to the lower probability axis. The blue wavy line on each axis represented the data distribution of this factor; Receiver operating characteristic curve for the CAPS model and clinical factor model in Cohort 2 (B); Calibration plot of the CAPS model with a 1000 repetition bootstrap in Cohort 2 (C); Decision curve of the two prediction models showed the net benefit for the CAPS model was larger than that for the traditional clinical model (D); Clinical impact analysis curve of CAPS visually showed the number of people classified as positive (high-risk) by the model and the number of true positive people under each threshold probability (E); Receiver operating characteristic curve for the external validation of CAPS model in Cohort 3 (F); Calibration plot for the external validation of CAPS model in Cohort 3 (G). CPB time: cardiopulmonary bypass time; MRBC: massive transfusion of red blood cells; CAPS: the combined CPB-ARDS prediction score; ROC: receiver operating characteristic curve; 95% CI: 95% confidence interval.

Table 2

The results of F1 score, precision, sensitivity, specificity, and AUC (95% CI) after *N*-fold cross-validation of clinical factor prediction models and the CAPS models.

Prediction model	Clinical factors model	CAPS model
Features	CPB time, MRBC, age, ultrafiltration volume	TXNDC5, CTSL, NPC2, CPB time, MRBC
Precision	76.19%	83.33%
Sensitivity	85.33%	93.33%
Specificity	47.36%	61.16%
F1 score	80.50%	88.05%
AUC (95% CI)		
3-fold	0.738 (0.730, 0.747)	0.832 (0.825, 0.839)
5-fold	0.730 (0.715, 0.745)	0.835 (0.824, 0.845)
10-fold	0.740 (0.722, 0.757)	0.839 (0.824, 0.855)

AUC, area under the receiver operating characteristic curve; CAPS, the combined CPB-ARDS prediction score; CPB time, time of cardiopulmonary bypass; MRBC, massive transfusion of red blood cells.

the plasma of CPB-ARDS patients. The possible causes could be increased synthesis and secretion by the liver[42] and reduced renal degradation or clearance[41].

Strengths and limitations

Our study has numerous strengths. First, the study originality resides in its design (going from supervised bedside-omics screening to the target organ and bench analysis), involving two different species (humans and rats). Second, the cases and controls in the nested cohort study were selected from the same cohort. The population is therefore homogeneous and comparable, which can better control the selection bias. In addition, nested cohort studies are more economical and time-saving than cohort studies, as not all biological samples in the cohort need to be detected. Third, we collected both clinical and protein data and developed a machine learning-based prediction system with better performance than traditional clinical factor models. Finally, these DEPs at both preoperative and postoperative timepoints indicated early dynamic changes in protein markers.

There are also some limitations. The first limitation of this study derives from its single-center design. The fact that biomarkers from the proteomics results were further validated by ELISA using a larger cohort contributed to the confidence in the results. Second, the number of DEPs in the plasma proteomics of this study was limited. For the purpose of early prediction, we detected proteomic differences before the onset of ARDS, in which the changes in protein expression may be at the early stage. The third limitation comes from the absence of lung tissues from patients, which precluded us from assessing the differential expression of biomarkers in the lung. Although, we established rat LIRI models and detected the expression of related proteins in rat lung tissue, we could not completely restore the clinical background of patients undergoing CPB.

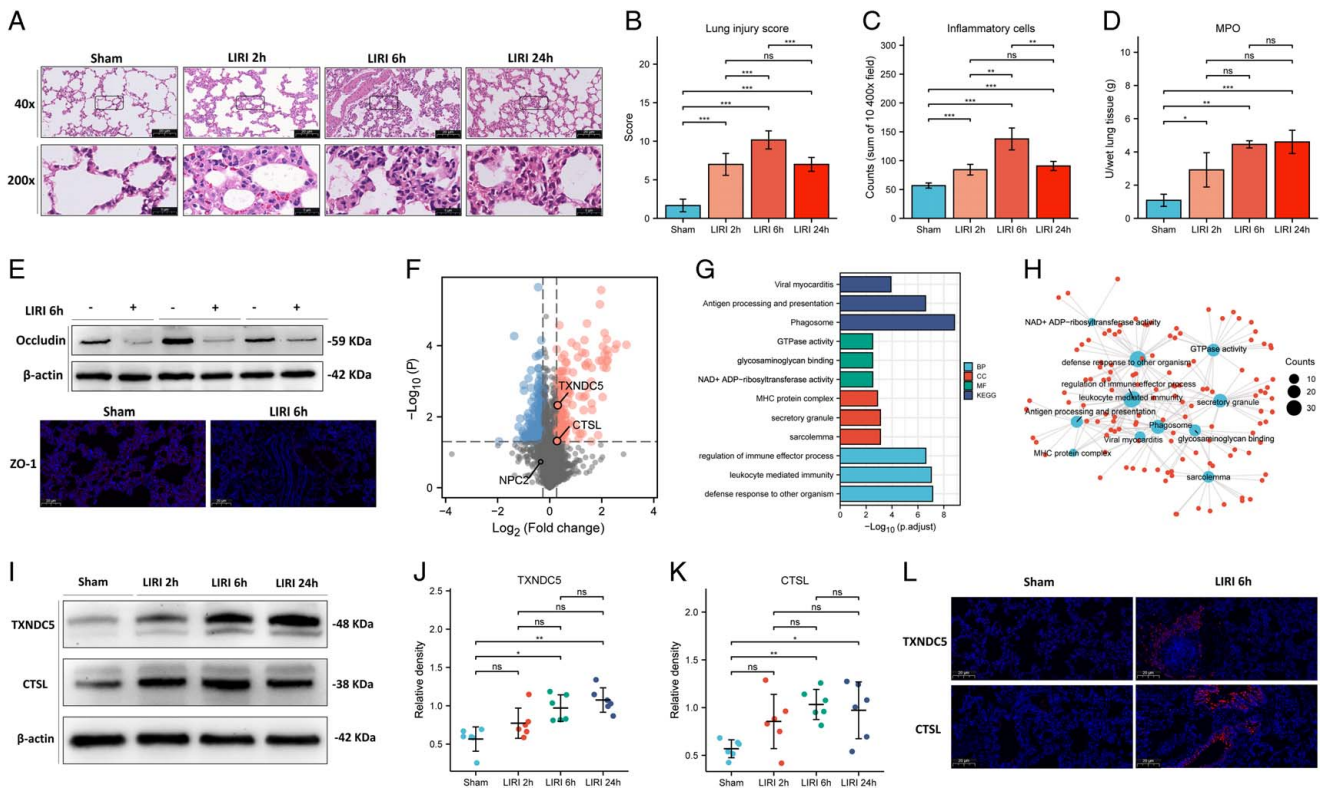

Figure 6. The expression and function of the targeted protein predictors in LIRI rat model. The degree of lung injury after 2, 6, and 24 h of reperfusion, including the hematoxylin-eosin staining (A), lung injury score (B), the amount of inflammatory cells (C), and the expression of MPO (D); The immunoblot of Occludin and immunofluorescence of ZO-1 (E); The volcano plot of altered protein expression in lung tissue of LIRI rats (F); The GO and KEGG enriched items (G, H); The Immunoblot (I) and quantification of the signal of the protein expression of TXNDC5 (J), and CTSL (K) in the lung tissues; The immunofluorescence of the protein expression of TXNDC5 and CTSL (L) in the lung tissues. Each bar represents the Mean ± SD; ns: $P \geq 0.05$; *$P < 0.05$; **$P < 0.01$; ***$P < 0.001$.

Conclusion

In conclusion, our study is one of the few proteomics studies to examine predictive biomarkers in ARDS, establish and externally validate a prediction model for the prediction of ARDS after CPB surgery. The use of a composite of clinical and protein predictors may play an important role in early therapeutics or preventative approaches for ARDS. Additionally, the early increase in TXNDC5 and CTSL may be related to endothelial and vascular injury and provides potential therapeutic targets for this syndrome. Further explorations are needed to elucidate the implicated mechanisms of predictive biomarker interactions underlying CPB-ARDS.

Ethical approval

For the clinical study protocol, it was set in compliance with Helsinki Declaration and was approved by the Institutional Review Board of the Wuhan Union Hospital (Approval No. 20200518) on 13 January 2021.

Consent

Written informed consent was obtained from each patient or legal guardian before enrollment. For the animal experiment protocol, it was in accordance with ARRIVE guidelines and approved by Experimental Animal Center of Tongji Medical College (IACUC No. 2916).

Sources of funding

This research was supported by Hubei Technological Innovation Special Fund (2019ACA167).

Author contribution

Y.W., L.C., and C.Y.: formal analysis, investigation, and writing – original draft; T.W.: conceptualization; J.W. and S.Y.: supervision; B.L., H.X., S.H., F.W., and S.W.: investigation; S.H.: formal analysis; Y.L.: conceptualization, methodology, writing – review and editing, and project administration; N.D.: conceptualization, methodology, writing – review and editing, supervision; S.Y.: conceptualization, methodology, writing – review and editing, supervision, and funding acquisition. All authors have reviewed the article, revised it critically for important intellectual content, and approved the final manuscript.

Conflicts of interest disclosure

The authors declared that they have no conflicts of interest.

Research registration unique identifying number (UIN)

1. Name of the registry: clinicaltrials.gov.
2. Unique identifying number or registration ID: NCT04696172.
3. Hyperlink to your specific registration: https://clinicaltrials.gov/ct2/show/NCT04696172?term=NCT04696172&draw=2&rank=1.

Guarantor

Shanglong Yao.

Data availability statement

All data, models, and code used during the study are available from the corresponding author (Shanglong Yao, yaoshanglong@hust.edu.cn) by request.

Provenance and peer review

Not commissioned, externally peer-reviewed.

References

[1] Bronicki RA, Hall M. Cardiopulmonary bypass-induced inflammatory response: pathophysiology and treatment. Pediatr Crit Care Med 2016;17:S272–8.
[2] Stephens RS, Shah AS, Whitman GJ. Lung injury and acute respiratory distress syndrome after cardiac surgery. Ann Thorac Surg 2013;95:1122–9.
[3] Sanfilippo F, Palumbo GJ, Bignami E, *et al*. Acute respiratory distress syndrome in the perioperative period of cardiac surgery: predictors, diagnosis, prognosis, management options, and future directions. J Cardiothorac Vasc Anesth 2022;36:1169–79.
[4] Rubenfeld GD, Caldwell E, Peabody E, *et al*. Incidence and outcomes of acute lung injury. N Engl J Med 2005;353:1685–93.
[5] Buggeskov KB, Gronlykke L, Risom EC, *et al*. Pulmonary artery perfusion versus no perfusion during cardiopulmonary bypass for open heart surgery in adults. Cochrane Database Syst Rev 2018;2:D11098.
[6] Matthay MA, Mcauley DF, Ware LB. Clinical trials in acute respiratory distress syndrome: challenges and opportunities. Lancet Respir Med 2017;5:524–34.
[7] Spragg RG, Bernard GR, Checkley W, *et al*. Beyond mortality: future clinical research in acute lung injury. Am J Respir Crit Care Med 2010;181:1121–7.
[8] Kor DJ, Lingineni RK, Gajic O, *et al*. Predicting risk of postoperative lung injury in high-risk surgical patients: a multicenter cohort study. Anesthesiology 2014;120:1168–81.
[9] Gajic O, Dabbagh O, Park PK, *et al*. Early identification of patients at risk of acute lung injury: evaluation of lung injury prediction score in a multicenter cohort study. Am J Respir Crit Care Med 2011;183:462–70.
[10] Ranieri VM, Rubenfeld GD, Thompson BT, *et al*. Acute respiratory distress syndrome: the Berlin Definition. JAMA 2012;307:2526–33.
[11] Garcia-Laorden MI, Lorente JA, Flores C, *et al*. Biomarkers for the acute respiratory distress syndrome: how to make the diagnosis more precise. Ann Transl Med 2017;5:283.
[12] Samanta J, Singh S, Arora S, *et al*. Cytokine profile in prediction of acute lung injury in patients with acute pancreatitis. Pancreatology 2018;18:878–84.
[13] Wang YM, Qi X, Gong FC, *et al*. Protective and predictive role of Mucin1 in sepsis-induced ALI/ARDS. Int Immunopharmacol 2020;83:106438.
[14] Alladina JW, Levy SD, Hibbert KA, *et al*. Plasma concentrations of soluble suppression of Tumorigenicity-2 and Interleukin-6 are predictive of successful liberation from mechanical ventilation in patients with the acute respiratory distress syndrome. Crit Care Med 2016;44:1735–43.
[15] Levitt JE, Rogers AJ. Proteomic study of acute respiratory distress syndrome: current knowledge and implications for drug development. Expert Rev Proteomics 2016;13:457–69.
[16] Agha R, Abdall-Razak A, Crossley E, *et al*. STROCSS 2019 guideline: strengthening the reporting of cohort studies in surgery. Int J Surg 2019;72:156–65.
[17] Kilkenny C, Browne WJ, Cuthill IC, *et al*. Improving bioscience research reporting: the ARRIVE guidelines for reporting animal research. Plos Biol 2010;8:e1000412.
[18] English JA, Lopez LM, O'Gorman A, *et al*. Blood-based protein changes in childhood are associated with increased risk for later psychotic disorder: evidence from a nested case-control study of the ALSPAC longitudinal birth cohort. Schizophr Bull 2018;44:297–306.

[19] Li T, Luo N, Du L, *et al*. Early and marked up-regulation of TNF-alpha in acute respiratory distress syndrome after cardiopulmonary bypass. Front Med 2012;6:296–301.
[20] Mazzeffi M, Kassa W, Gammie J, *et al*. Preoperative aspirin use and lung injury after aortic valve replacement surgery: a retrospective cohort study. Anesth Analg 2015;121:271–7.
[21] Chen SW, Chang CH, Chu PH, *et al*. Risk factor analysis of postoperative acute respiratory distress syndrome in valvular heart surgery. J Crit Care 2016;31:139–43.
[22] Xie J, Liu L, Yang Y, *et al*. A modified acute respiratory distress syndrome prediction score: a multicenter cohort study in China. J Thorac Dis 2018; 10:5764–73.
[23] Trillo-Alvarez C, Cartin-Ceba R, Kor DJ, *et al*. Acute lung injury prediction score: derivation and validation in a population-based sample. Eur Respir J 2011;37:604–9.
[24] Webb-Robertson BJ, Wiberg HK, Matzke MM, *et al*. Review, evaluation, and discussion of the challenges of missing value imputation for mass spectrometry-based label-free global proteomics. J Proteome Res 2015; 14:1993–2001.
[25] Maltesen RG, Wimmer R, Rasmussen BS. A longitudinal serum NMR-based metabolomics dataset of ischemia-reperfusion injury in adult cardiac surgery. Sci Data 2020;7:198.
[26] Saito M, Chen-Yoshikawa TF, Suetsugu K, *et al*. Pirfenidone alleviates lung ischemia-reperfusion injury in a rat model. J Thorac Cardiovasc Surg 2019;158:289–96.
[27] Jiang J, Huang K, Xu S, *et al*. Targeting NOX4 alleviates sepsis-induced acute lung injury via attenuation of redox-sensitive activation of CaMKII/ERK1/2/MLCK and endothelial cell barrier dysfunction. Redox Biol 2020;36:101638.
[28] Li J, Lu K, Zhang X, *et al*. SIRT3-mediated mitochondrial autophagy in refeeding syndrome-related myocardial injury in sepsis rats. Ann Transl Med 2022;10:211.
[29] Shu T, Ning W, Wu D, *et al*. Plasma proteomics identify biomarkers and pathogenesis of COVID-19. Immunity 2020;53:1108–22.
[30] Wen XP, Zhang YZ, Wan QQ. Non-targeted proteomics of acute respiratory distress syndrome: clinical and research applications. Proteome Sci 2021;19:5.
[31] Kor DJ, Warner DO, Alsara A, *et al*. Derivation and diagnostic accuracy of the surgical lung injury prediction model. Anesthesiology 2011;115: 117–28.
[32] Agrawal A, Matthay MA, Kangelaris KN, *et al*. Plasma angiopoietin-2 predicts the onset of acute lung injury in critically ill patients. Am J Respir Crit Care Med 2013;187:736–42.
[33] Liu XW, Ma T, Cai Q, *et al*. Elevation of serum PARK7 and IL-8 levels is associated with acute lung injury in patients with severe sepsis/septic shock. J Intensive Care Med 2019;34:662–8.
[34] Lee TH, Yeh CF, Lee YT, *et al*. Fibroblast-enriched endoplasmic reticulum protein TXNDC5 promotes pulmonary fibrosis by augmenting TGFbeta signaling through TGFBR1 stabilization. Nat Commun 2020; 11:4254.
[35] Shih YC, Chen CL, Zhang Y, *et al*. Endoplasmic reticulum protein TXNDC5 augments myocardial fibrosis by facilitating extracellular matrix protein folding and redox-sensitive cardiac fibroblast activation. Circ Res 2018;122:1052–68.
[36] Zhao MM, Yang WL, Yang FY, *et al*. Cathepsin L plays a key role in SARS-CoV-2 infection in humans and humanized mice and is a promising target for new drug development. Signal Transduct Target Ther 2021;6:134.
[37] Nie X, Qian L, Sun R, *et al*. Multi-organ proteomic landscape of COVID-19 autopsies. Cell 2021;184:775–91.
[38] Tang TT, Lv LL, Pan MM, *et al*. Hydroxychloroquine attenuates renal ischemia/reperfusion injury by inhibiting cathepsin mediated NLRP3 inflammasome activation. Cell Death Dis 2018;9:351.
[39] He W, Mccarroll CS, Nather K, *et al*. Inhibition of myocardial cathepsin-L release during reperfusion following myocardial infarction improves cardiac function and reduces infarct size. Cardiovasc Res 2022;118:1535–47.
[40] Ko DC, Binkley J, Sidow A, *et al*. The integrity of a cholesterol-binding pocket in Niemann-Pick C2 protein is necessary to control lysosome cholesterol levels. Proc Natl Acad Sci USA 2003;100:2518–25.
[41] Bai Y, Yin S, Gbordzor V, *et al*. Increase in plasma Niemann-Pick disease type C2 protein is associated with poor prognosis of sepsis. Sci Rep 2021; 11:5907.
[42] Klein A, Amigo L, Retamal MJ, *et al*. NPC2 is expressed in human and murine liver and secreted into bile: potential implications for body cholesterol homeostasis. Hepatology 2006;43:126–33.